

See discussions, stats, and author profiles for this publication at: <https://www.researchgate.net/publication/221871916>

FCl:PCX complexes: Old and new types of halogen bonds

ARTICLE in THE JOURNAL OF PHYSICAL CHEMISTRY A · MARCH 2012

Impact Factor: 2.69 · DOI: 10.1021/jp211451y · Source: PubMed

CITATIONS

22

READS

76

4 AUTHORS, INCLUDING:



Ibon Alkorta

Spanish National Research Council

679 PUBLICATIONS 12,389 CITATIONS

SEE PROFILE



Goar Sánchez

University College Dublin

69 PUBLICATIONS 900 CITATIONS

SEE PROFILE



José Elguero

Spanish National Research Council

1,502 PUBLICATIONS 22,151 CITATIONS

SEE PROFILE

FCl:PCX Complexes: Old and New Types of Halogen Bonds

Ibon Alkorta,* Goar Sanchez-Sanz, and José Elguero

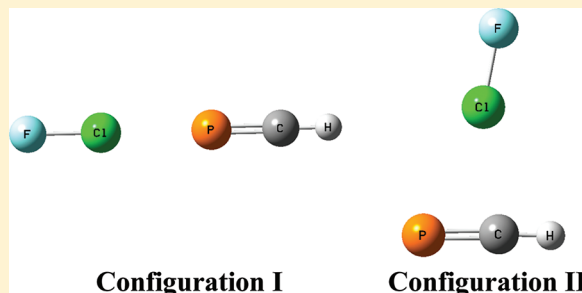
Instituto de Química Médica (CSIC), Juan de la Cierva, 3, 28006 Madrid, Spain

Janet E. Del Bene*

Department of Chemistry, Youngstown State University, Youngstown, Ohio 44555, United States

S Supporting Information

ABSTRACT: MP2/aug'-cc-pVTZ calculations have been performed to investigate the halogen-bonded complexes FCl:PCX, for X = NC, CN, F, H, CCH, CCF, CH₃, Li, and Na. Although stable complexes with a F–Cl...P halogen bond exist that form through the lone pair at P (configuration I), except for FCl:PCCN, the more stable complexes are those in which FCl interacts with the C≡P triple bond through a perturbed π system (configuration II). In complexes I, the nature of the halogen bond changes from traditional to chlorine-shared and the interaction energies increase, as the electron-donating ability of X increases. The anionic complex FCl:PC[−] has a chlorine-transferred halogen bond. SAPT analyses indicate that configuration I complexes with traditional halogen bonds are stabilized primarily by the dispersion interaction. The electrostatic interaction is the most important for configuration I complexes with chlorine-shared halogen bonds and for configuration II complexes except for FCl:PCNa for which the induction term is most important. The F–Cl stretching frequency is red-shifted upon complexation. EOM-CCSD/(qzp,qz2p) spin–spin coupling constants have been obtained for all FCl:PCX complexes with configuration I. ¹J(F–Cl) decreases upon complexation. ²XJ(F–P) values are quadratically dependent upon the F–P distance and are very sensitive to halogen-bond type. ¹XJ(Cl–P) tends to increase as the Cl–P distance decreases but then decreases dramatically in the chlorine-transferred complex FCl:PC[−] as the Cl–P interaction approaches that of a covalent Cl–P bond. Values of ¹J(F–Cl) for configuration II are reduced relative to configuration I, reflecting the longer F–Cl distances in II compared to those of the neutral complexes of I. Although the F–P and Cl–P distances in configuration II complexes are shorter than these distances in the corresponding configuration I complexes, ²XJ(F–P) and ¹XJ(Cl–P) values are significantly reduced, indicating that coupling through the perturbed C–P π bond is less efficient. The nature of F–P coupling for configuration II is also significantly different, as evidenced by the relative importance of PSO, FC, and SD components.



■ INTRODUCTION

Methyldiylne phosphane (HCP), also known as methinophosphide and phosphaethyne, was synthesized for the first time in 1961 by Gier working at the Du Pont Co. in Delaware,¹ and was the first molecule reported with a triple bond between carbon and phosphorus. This molecule is present in the interstellar medium and in the atmosphere of Saturn.² The ground-state geometry of the HCP molecule deduced from microwave spectroscopy is linear with $C_{\infty v}$ symmetry.³

Due to the simplicity of its structure and the fact that HCP is the phosphorus analog of HCN, this molecule has been investigated extensively both experimentally and theoretically. Experimental chemical studies are well summarized in Regitz's review.⁴ The most significant theoretical studies concerning the reactivity of HCP are those of Nguyen⁵ and of Schleyer.⁶ An important group of publications are devoted to various spectroscopic studies including electronic,⁷ vibrational–rotational,⁸ Raman,⁹ microwave and lower-energy regions,^{10,11} SEP (stimulated emission pumping),¹² and NMR.¹³ Theoretical studies range from Hartree–Fock calculations¹⁴ to multi-

reference CI,¹⁵ MP4SDQ,¹⁶ CASSCF,¹⁷ RMP2,¹⁸ CISD,¹⁹ and CCSD(T).²⁰ We have reported studies of protonation and hydrogen bond formation involving HCP.^{21,22}

In previous studies we have also examined halogen-bonded binary and ternary complexes formed from HCN (hydrogen cyanide) and HNC (hydrogen isocyanide), as well as derivatives of these molecules.^{23–26} Neutral complexes of FCl with XCN as the base are stabilized by traditional halogen bonds. In contrast, traditional, chlorine-shared, and chlorine-transferred ion-pair halogen bonds are found in neutral complexes with XNC. In these complexes, the type of halogen bond depends on the nature of the substituent X. As an extension of those studies, we now turn to complexes formed by XCP as the base in halogen-bonded complexes FCl:PCX, for X = NC, CN, F, H, CCH, CCF, CH₃, Li, and Na, and including the anionic complex FCl:PC[−]. We inquire about the nature of

Received: November 28, 2011

Revised: January 27, 2012

Published: February 29, 2012

the halogen bonds and investigate the structures, binding energies, bonding, and selected spectroscopic properties of these complexes.

■ COMPUTATIONAL DETAILS

The geometries of monomers and complexes have been optimized at MP2 with the aug'-cc-pVTZ basis set,²⁷ which is the Dunning aug-cc-pVTZ basis^{28,29} for the heavy atoms and the cc-pVTZ basis set for H atoms. Frequency calculations at the same computational level have been carried out to determine whether these optimized complexes are local minima or transition structures on their potential surfaces. These calculations have been carried out with the Gaussian-09 program.³⁰

The SAPT (symmetry adapted perturbation theory)³¹ method allows for the decomposition of the interaction energy into different terms related to physically well-defined components, such as those arising from electrostatic, exchange, induction, and dispersion terms. The interaction energy can be expressed within the framework of the SAPT method as

$$E_{\text{int}} = E_{\text{el}}^{(1)} + E_{\text{exch}}^{(1)} + E_{\text{i}}^{(2)} + E_{\text{D}}^{(2)} \quad (1)$$

where $E_{\text{el}}^{(1)}$ is the electrostatic interaction energy of the monomers each with its unperturbed electron distribution; $E_{\text{exch}}^{(1)}$ is the first-order exchange energy term; $E_{\text{i}}^{(2)}$ denotes the second-order induction energy arising from the interaction of permanent multipoles with induced multipole moments and charge-transfer contributions, plus the change in the repulsion energy induced by the deformation of the electronic clouds of the monomers; and $E_{\text{D}}^{(2)}$ is the second-order dispersion energy, which is related to the instantaneous multipole-induced multipole moment interactions plus the second-order correction for coupling between the exchange repulsion and the dispersion interactions.

The DFT-SAPT formulation has been used to investigate interaction energies. In this approach, the energies of interacting monomers are expressed in terms of orbital energies obtained from Kohn–Sham density functional theory.^{32,33} In addition to the terms listed in eq 1, a Hartree–Fock correction term $\delta(\text{HF})$, which includes higher-order induction and exchange corrections, has been included.³⁴ The DFT-SAPT calculations have been performed with the MOLPRO program³⁵ using the PBE0/aug'-cc-pVTZ computational method.³⁶

The electron densities of monomers and complexes have been analyzed employing the atoms in molecules (AIM) methodology^{37,38} with the AIMAll program.³⁹ A value of 0.001 e/bohr³ has been used to define van der Waals surfaces. The TOPMOD program⁴⁰ has been used to analyze the areas of electron concentration in terms of the Electron Localization Function (ELF).⁴¹

Spin–spin coupling constants for monomers and complexes were computed using the equation-of-motion coupled cluster singles and doubles (EOM-CCSD) method in the CI-(configuration interaction)-like approximation,^{42,43} with all electrons correlated. For these calculations, the Ahlrichs⁴⁴ qzp basis set was placed on ¹³C, ¹⁵N, and ¹⁹F atoms, and the qz2p basis set on ³¹P and ³⁵Cl. A previously developed corresponding basis set with the same number of functions as the qzp basis was placed on ⁷Li.⁴⁵ The Dunning cc-pVDZ basis was placed on ¹H atoms.²⁸ Because a corresponding qz2p basis set is not available for Na, no coupling constants have been computed for

FCI:PCNa complexes. Coupling constants have been evaluated as a sum of four terms: the paramagnetic spin–orbit (PSO), diamagnetic spin–orbit (DSO), Fermi-contact (FC), and spin-dipole (SD).⁴⁶ The coupling constant calculations were carried out using ACES II⁴⁷ on the IBM 1350 cluster (Glenn) at the Ohio Supercomputer Center.

■ RESULTS AND DISCUSSION

Electronic Properties of PCX Molecules. PCX molecules have $C_{\infty v}$ symmetry (C_{3v} for PCCH_3) giving a linear $\text{P}\equiv\text{C}-\text{A}$ arrangement, with A the atom of the substituent X that is bonded to C. Because PCH is the parent molecule in this series, we have explored in detail its electronic characteristics, beginning with its molecular electrostatic potential (MEP), which is illustrated in Figure 1. Figure 1 shows a negatively

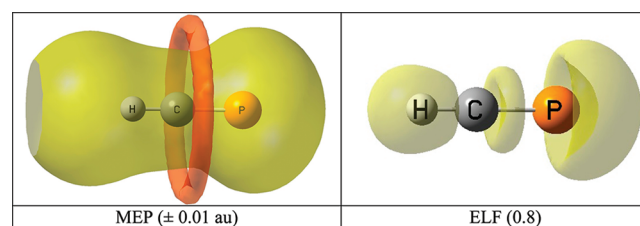


Figure 1. MP2/aug'-cc-pVTZ molecular electrostatic potential and ELF of the PCH molecule. In the MEP, orange and yellow correspond to negative and positive regions, respectively. The ELF isosurface is at 0.8.

charged toroidal region surrounding the $\text{C}\equiv\text{P}$ triple bond. The toroid is shifted toward the carbon atom, with -0.014 au as its largest negative value. The electrostatic potential at the van der Waals 0.001 au surface along the C–P bond axis on the lone-pair side of the C–P bond is positive.

The representation of the ELF in Figure 1 also shows a toroidal region consistent with a $\text{C}\equiv\text{P}$ triple bond. In addition, the region associated with the lone pair on P indicates that the electron cloud is widely dispersed. These descriptions are in agreement with the results of a previous study, which showed that PCH and PCCH_3 do not form proton-bound complexes through the P lone pair,^{21,22} but through the $\text{P}\equiv\text{C}$ triple bond. Moreover, in some cases, protonation of these monomers leads to a nonclassical cation.^{21,48}

Replacement of H by a substituent X modulates the electronic properties of the C–P bond, the extent of which is determined by the nature of the substituent. The strong electron-donating substituents Li and Na lead to the formation of a new minimum, that is, a region in which the MEP is negative on the lone pair side of the C–P bond. In contrast, substitution of the electron-withdrawing groups CN and NC leads to a positive MEP in this region and an increased positive MEP around the C–P bond. Table 1 reports the values of the MEP minima and the values of the MEP along the PC bond axis at the van der Waals surfaces, which have an electron density of 0.001 au. On this surface, the MEP is negative only for $\text{X} = \text{CH}_3$, Li, and Na.

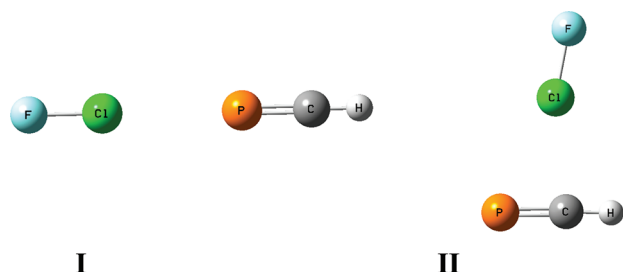
Halogen-Bonded Complexes. Structures and Energies. Two different configurations have been identified for complexes FCI:PCX. Configuration I has a linear $\text{F}-\text{Cl}\cdots\text{P}\equiv\text{C}$ arrangement with halogen bond formation occurring through the lone pair of electrons on P. Configuration II arises from halogen bond formation with the perturbed in-plane π cloud of the $\text{P}\equiv\text{C}$ triple bond. Complexes with configuration I

Table 1. MEP Minimum Values (au) around the C≡P Triple Bond and at the van der Waals (vdW) 0.001 au Surface on the Lone Pair Side of the C≡P Bond for Molecules PCX

| molecule | MEP min around the C≡P bond | MEP at vdW 0.001 au surface |
|-------------------|-----------------------------|-----------------------------|
| PCNC | <i>a</i> | 0.0223 |
| PCCN | <i>a</i> | 0.0355 |
| PCF | −0.0059 | 0.0186 |
| PCH | −0.0142 | 0.0093 |
| PCCCH | −0.0109 | 0.0128 |
| PCCCF | −0.0107 | 0.0129 |
| PCCH ₃ | −0.0184 | −0.0009 |
| PCLi | −0.0632 | −0.0347 |
| PCNa | −0.0758 | −0.0450 |

^aFor these two molecules, the MEP is positive.

Scheme 1. FCl:PCH Complexes with Configurations I and II



have $C_{\infty v}$ symmetry (C_{3v} for FCl:PCCH₃), whereas those with II have C_s symmetry. Configurations I and II for FCl:PCH are illustrated in Scheme 1.

Neutral complexes with X = H, CCH, CCF, and Li have two minima (I and II) on their potential surfaces. For these, II is more stable than I. Complexes with X = NC, F, CH₃, and Na have only a single minimum corresponding to configuration II, with configuration I having two degenerate imaginary frequencies. The complex FCl:PCCN has only configuration I as a minimum-energy structure. All attempts to optimize configuration II for this complex reverted spontaneously to configuration I.

What types of halogen bonds stabilize complexes with configuration I? Table 2 presents F–Cl and Cl–P distances and binding energies of complexes with configuration I, arranged according to increasing binding energy. It is apparent from Table 2 that these complexes can be subdivided into three types, based on binding energies and distances. The complexes from X = NC to X = CH₃ have binding energies ranging from 5 to 10 kJ mol^{−1}. For these, the increase in the F–Cl distance upon complexation is small, from 0.002 to 0.009 Å. These complexes are stabilized by traditional halogen bonds. The complexes FCl:PCLi and FCl:PCNa which have strong electron-donating substituents have significantly increased binding energies of 23 and 28 kJ mol^{−1}, respectively, and F–Cl distances that have increased by 0.041 and 0.069 Å, respectively. The Cl–P distances are also much shorter than the Cl–P distances in complexes with traditional halogen bonds. FCl:PCLi and FCl:PCNa are stabilized by chlorine-shared halogen bonds. Only when the phosphorus base is the anion PC[−] does chlorine transfer occur, to produce the complex F[−]:ClPC. This complex has a binding energy of 128 kJ mol^{−1} relative to FCl and PC[−]. The Cl–P bond length is 2.139

Table 2. F–Cl and Cl–P Distances (R, Å), Binding Energies (ΔE , kJ mol^{−1}), and Number of Imaginary Frequencies (NIMAG) for Complexes FCl:PCX with Configuration I^a

| complex | R(F–Cl) ^b | R(Cl–P) | ΔE^c | NIMAG |
|-----------------------|----------------------|--------------------|--------------|-------|
| FCl:PCNC | 1.641 | 3.209 | 4.80 | 2 |
| FCl:PCCN | 1.640 | 3.195 | 4.96 | 0 |
| FCl:PCF | 1.642 | 3.220 | 5.81 | 2 |
| FCl:PCH | 1.644 | 3.133 | 8.06 | 0 |
| FCl:PCCCH | 1.644 | 3.122 | 8.53 | 0 |
| FCl:PCCCF | 1.645 | 3.116 | 8.77 | 0 |
| FCl:PCCH ₃ | 1.647 | 3.080 | 10.42 | 2 |
| FCl:PCLi | 1.679 | 2.751 | 23.09 | 0 |
| FCl:PCNa | 1.707 | 2.609 | 27.84 | 2 |
| FCl:PC [−] | 2.032 | 2.139 ^d | 128.46 | 0 |

^aComplexes with NIMAG = 2 do not correspond to local minima.

^bThe F–Cl distance in the monomer is 1.638 Å. ^cBinding energies are the negative energies for the reaction FCl + PCX → FCl:PCX. ^dThe Cl–P distance in ClPC is 2.057 Å.

Å, which is only 0.082 Å longer than the bond length in the neutral molecule ClPC.

How do the changes seen in halogen bond type compare with those found in corresponding complexes FCl:NCX and FCl:CNX? Neutral complexes FCl:NCX are stabilized by traditional halogen bonds, whereas the complex FCl:NC[−] has a chlorine-shared halogen bond. All of these have linear F–Cl⋯N≡C arrangements and are minima on their potential surfaces. In contrast, neutral complexes FCl:CNX are stabilized by traditional, chlorine-shared, and chlorine-transferred ion-pair halogen bonds, with the type of halogen bond changing as the electron-donating ability of the substituent changes. All have linear F–Cl⋯C≡N arrangements and are also minima on their potential surfaces. The lone pairs on N of N≡C–X and on C of C≡N–X are much more localized than the lone pair on P. A comparison of the proton affinities of the parent molecules in each series shows HCP (699 kJ) < HCN (713 kJ) << HNC (772 kJ),⁴⁹ although HCP does not protonate at P.^{21,48} That the neutral complex FCl:CNH has a chlorine-shared halogen bond is consistent with the high proton affinity of CNH. The binding energies of configuration I complexes are quadratically related to the values of the MEP on the vdW surfaces along the PC bond axis for the corresponding monomers, as illustrated in Figure 2.

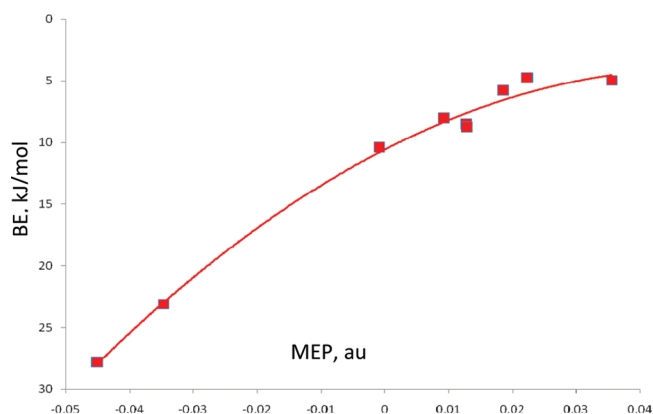


Figure 2. Binding energies (BE) of complexes with configuration I versus the MEP values of the corresponding isolated PCX molecules at the vdW surfaces from Table 1.

It is appropriate to ask why FCl:PCCN does not exist as a configuration II complex, because all other FCl:PCX complexes have configuration II as the more stable minimum on the halogen-bonding surface. As evident from Table 1, both PCCN and PCNC have positive values of the MEP around the $\text{C}\equiv\text{P}$ triple bond. This might suggest that neither PCNC nor PCCN would form stable configuration II complexes. This is the situation for FCl:PCCN, in which case it was not even possible to optimize a configuration II structure. In contrast, FCl:PCNC has configuration II as the equilibrium structure and I as a transition structure. Thus, the absence of a type II structure for FCl:PCCN cannot be attributed solely to the positive value of the MEP around the $\text{C}\equiv\text{P}$ triple bond. Rather, it may be related to the nature of the HOMO, which for all molecules PCX, is a pair of degenerate π orbitals. However, the π HOMOs are significantly more tightly bound in PCCN than in any other molecule, which might also contribute to the absence of a FCl:PCCN configuration II complex on the potential surface.

All neutral complexes FCl:PCX except for FCl:PCCN have the hydrogen-bonded π complex (configuration I) as the more stable minimum on the potential surface. Table 3 reports F–Cl,

Table 3. F–Cl, Cl–P, and Cl–C Distances (R , Å) and Binding Energies (ΔE , kJ mol^{-1}) for Complexes FCl:PCX with Configuration II^a

| complex | $R(\text{F–Cl})$ | $R(\text{Cl–P})$ | $R(\text{Cl–C})$ | ΔE^b |
|-----------------------|------------------|------------------|------------------|--------------|
| FCl:PCNC | 1.656 | 3.047 | 2.860 | 16.41 |
| FCl:PCCN ^c | | | | |
| FCl:PCF | 1.664 | 3.005 | 2.804 | 19.40 |
| FCl:PCH | 1.667 | 3.032 | 2.724 | 21.39 |
| FCl:PCCCH | 1.666 | 2.982 | 2.816 | 21.67 |
| FCl:PCCCF | 1.668 | 2.972 | 2.807 | 22.54 |
| FCl:PCCH ₃ | 1.685 | 2.889 | 2.650 | 29.23 |
| FCl:PCLi | 1.826 | 2.626 | 2.374 | 79.07 |
| FCl:PCNa | 2.697 | 2.154 | 1.983 | 158.39 |

^aComplexes reported in this table are minima on their potential surfaces. ^bBinding energies are the negative energies for the reaction $\text{FCl} + \text{PCX} \rightarrow \text{FCl:PCX}$. ^cA complex with configuration II could not be optimized.

Cl–P, and Cl–C distances and binding energies for these complexes. In complexes from FCl:PCNC to FCl:PCCH₃, the Cl–P distance decreases by 0.158 Å and the Cl–C distance decreases by 0.210 Å as the binding energy increases from 16 to 29 kJ mol^{-1} . Thus, the complexes in this set are structurally and energetically similar. However, dramatic changes are seen in the structures and binding energies of the complexes FCl:PCLi and FCl:PCNa. The strong electron-donating substituents lead to much longer F–Cl and shorter Cl–P and Cl–C distances, and increased binding energies of 79 and 158 kJ mol^{-1} , respectively. These large interaction energies arise from the chlorine-transferred nature of these complexes, which results in significant distortion of the PCLi and PCNa molecules, as illustrated in Figure 3.

SAPT Analyses. Data from the SAPT analyses are reported in Table S3 of the Supporting Information. The SAPT interaction energies for complexes with configuration I are significantly less than the MP2 binding energies of these complexes. Indeed, the SAPT data indicate that FCl:PCCN is not a bound complex! For complexes with configuration I, the largest contribution to the SAPT energy comes from the destabilizing exchange term.

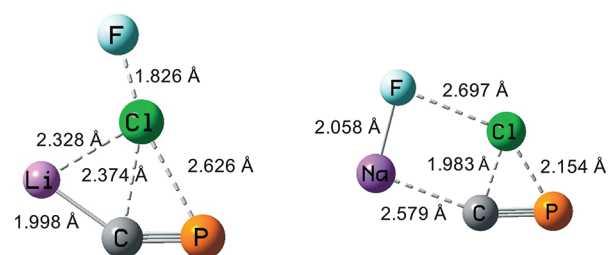


Figure 3. MP2/aug-cc-pVTZ optimized geometries of FCl:PCLi and FCl:PCNa with configuration II, illustrating the chlorine-transferred nature of the bonding and the distortion of the PCLi and PCNa molecules.

However, except for FCl:PCCN, the remaining terms summed together account for the stability of these complexes. For those complexes with traditional halogen bonds, the most important stabilizing interaction arises from dispersion, followed by the $\delta(\text{HF})$ term for the three most weakly bound complexes, and by the electrostatic term for the remaining complexes. This term becomes increasingly more important as the binding energy increases.

Changing the halogen bond type from traditional to chlorine-shared causes dramatic changes in the relative importance of the various SAPT terms. Although the exchange term, which is destabilizing, still makes the largest contribution, the electrostatic term is now by far the largest stabilizing interaction. The dispersion and $\delta(\text{HF})$ terms are similar and next in importance, followed by the induction term which is significantly larger in the complex FCl:PCNa than in FCl:PCLi.

For complexes with configuration II, the destabilizing exchange term still is the largest of the interaction terms. The most important attractive contribution comes from the electrostatic term, except for the FCl:PCNa complex for which the induction term is more important. The dispersion and $\delta(\text{HF})$ terms tend to be similar in the more weakly bound complexes. Complexes FCl:PCLi and FCl:PCNa are characterized by dramatic increases in the absolute values of all interaction terms. The changes in the interaction terms for these two complexes reflect their unusual structures, as illustrated in Figure 3.

Electron Density Analyses. The AIM topological analyses of the electron densities show the presence of intermolecular bond critical points (BCPs) in all complexes. In complexes with configuration I, the bond path connects the Cl and P atoms, whereas those with configuration II have a curved bond path connecting the Cl and C atoms, as illustrated in Figure 4. Values of the electron densities (ρ_{BCP}) and Laplacians ($\nabla^2\rho_{\text{BCP}}$) at bond critical points are reported in Table S4 of the Supporting Information. Small values of ρ_{BCP} and positive values of the $\nabla^2\rho_{\text{BCP}}$ are the norm, except for the anionic complex with PC^- in which case $\nabla^2\rho_{\text{BCP}}$ becomes negative, consistent with the covalent bond character of the Cl–P bond. Exponential relationships are found between interatomic distances of the atoms involved in the intermolecular interaction and values of ρ_{BCP} , consistent with relationships found for other weak interactions.^{50–52}

F–Cl Stretching Frequencies. The calculated harmonic stretching frequency of the isolated FCl molecule (800 cm^{-1}) nicely reproduces the experimental value of 783 cm^{-1} .⁵³ Complexation produces an elongation of the F–Cl bond, and this leads to a red shift of the FCl stretching frequency, as evident from the data of Table 4. The shift is greater in

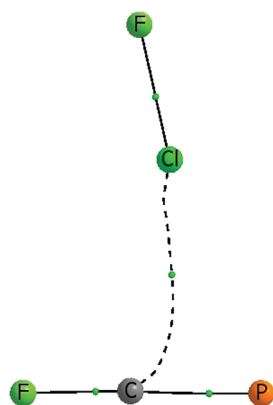


Figure 4. Molecular graph of the FCl:PCF complex with configuration II, showing the intermolecular bond path and the positions of BCPs.

Table 4. MP2/aug'-cc-pVTZ F-Cl Red Shifts of Harmonic Stretching Frequencies (cm^{-1}) for Complexes FCl:PCX with Configurations I and II^a

| complex | $\Delta\nu_{\text{F-Cl}}$ for I | $\Delta\nu_{\text{F-Cl}}$ for II |
|-----------------------|---------------------------------|----------------------------------|
| FCl:PCNC | -12 | -46 |
| FCl:PCCN | -13 | |
| FCl:PCF | -13 | -84 |
| FCl:PCH | -22 | -80 |
| FCl:PCCCH | -22 | -91 |
| FCl:PCCCF | -22 | -96 |
| FCl:PCCH ₃ | -28 | -142 |
| FCl:PCLi | -123 | <i>b</i> |
| FCl:PCNa | -194 | <i>b</i> |
| FCl:PC ⁻ | -447 ^c | |

^aThe computed F-Cl stretching frequency in the monomer is 800 cm^{-1} . ^bIn these complexes the F-Cl stretch is highly coupled to other vibrations due to the unusual and distinctive structures of these complexes. ^cThis low-frequency stretch is associated with the ion F⁻ and the Cl atom of ClPC.

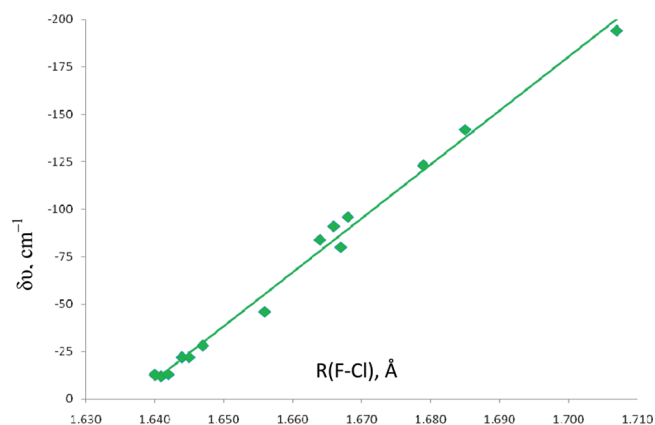


Figure 5. Red shift of the F-Cl stretching frequency ($\delta\nu$) for neutral FCl:PCX complexes with configurations I and II versus the F-Cl distance.

complexes with configuration II than in the corresponding complexes with configuration I, because the former are more strongly bound and the F-Cl distances are longer. A linear relationship with a correlation coefficient of 0.992 is obtained between the red shift of the F-Cl stretching band of neutral complexes and the F-Cl distance, as illustrated in Figure 5. However, it should be noted that the potential surfaces along

the F-Cl stretching coordinate in complexes FCl:PCLi and FCl:PCNa of type I with chlorine-shared halogen bonds are relatively flat. This would give rise to larger anharmonicity corrections and somewhat lower F-Cl stretching frequencies for these two complexes.⁵⁴

Spin-Spin Coupling Constants for Complexes with Configuration I. Spin-spin coupling constants across F-Cl...P halogen bonds have been computed for FCl:PCX complexes with configuration I. Values of $^1J(\text{F-Cl})$, $^{1X}J(\text{Cl-P})$, and $^{2X}J(\text{F-P})$ are given in Table 5, and the components of these coupling constants are given in Table S5 of the Supporting Information.

Table 5. $^1J(\text{F-Cl})$, $^{2X}J(\text{F-P})$, and $^{1X}J(\text{Cl-P})$ (Hz) for Complexes FCl:PCX with Configuration I, and Selected Monomers

| complexes | $^1J(\text{F-Cl})$ | $^{2X}J(\text{F-P})$ | $^{1X}J(\text{Cl-P})$ |
|-----------------------|--------------------|----------------------|-----------------------|
| FCl:PCNC | 783.7 | 23.1 | 119.4 |
| FCl:PCCN | 782.7 | 21.9 | 118.4 |
| FCl:PCF | 788.6 | 24.1 | 121.3 |
| FCl:PCH | 782.2 | 41.3 | 144.3 |
| FCl:PCCCH | 783.8 | 40.8 | 149.9 |
| FCl:PCCCF | 781.4 | 42.0 | 152.6 |
| FCl:PCCH ₃ | 781.3 | 57.7 | 169.6 |
| FCl:PCLi | 764.8 | 232.8 | 309.0 |
| FCl:PC ⁻ | 568.0 | 448.1 | 23.6 |
| monomers | $^1J(\text{F-Cl})$ | | $^{1X}J(\text{Cl-P})$ |
| FCl | 798.4 | | |
| ClPCLi ⁺ | | | -240.4 |
| ClPC | | | -262.6 |

$^1J(\text{F-Cl})$. As evident from Table 1, complex formation leads to a decrease in $^1J(\text{F-Cl})$ relative to the monomer. $^1J(\text{F-Cl})$ correlates linearly with the F-Cl distance, with a correlation coefficient of 0.996. The excellent correlation is fortuitous because the inclusion of $^1J(\text{F-Cl})$ for the anion extends both the $^1J(\text{F-Cl})$ and $R(\text{F-Cl})$ scales and masks the variation in this coupling constant in the neutral complexes. When the anionic complex is removed, the correlation between $^1J(\text{F-Cl})$ and the F-Cl distance becomes quadratic and shows some scatter as evident from the reduced correlation coefficient of 0.82.

Table S5 of the Supporting Information shows that $^1J(\text{F-Cl})$ for the FCl monomer and all of the neutral complexes with traditional halogen bonds are dominated by a positive PSO term. The second largest contribution comes from the SD term, which is also positive. The FC term makes a much smaller contribution, and is negative. The smallest absolute values of these three terms are found for the FCl:PCLi complex, which has a chlorine-shared halogen bond with the longest F-Cl distance and the greatest binding energy. However, the nature of the F-Cl coupling changes dramatically in FCl:PC⁻ with its chlorine-transferred bond. In this complex, it is the positive FC term that dominates, followed by a positive PSO term, with a smaller positive contribution from the SD term.

$^{2X}J(\text{F-P})$. $^{2X}J(\text{F-P})$ values for configuration I complexes are reported in Table 5, and Figure 6 shows the dependence of this coupling constant on the F-P distance. The dependence is similar to the dependence of $^{2h}J(\text{X-Y})$ on the X-Y distance in complexes with X-H...Y hydrogen bonds.⁵⁵ The two points that are removed from the cluster of points in this figure belong to FCl:PCLi and FCl:PC⁻. These points are distinctive and

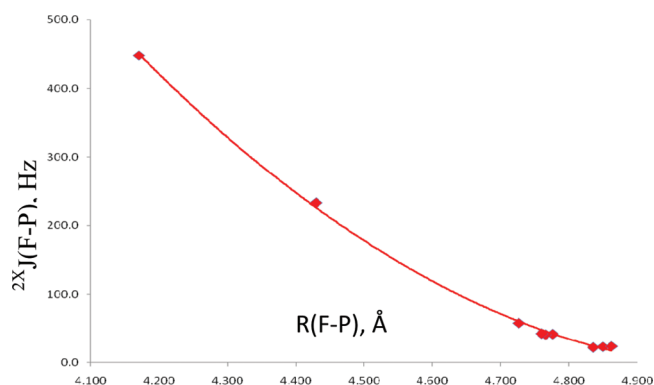


Figure 6. $^{2X}J(\text{F-P})$ versus the F-P distance for complexes with configuration I. The correlation coefficient is 0.998.

reflect the change in halogen-bond type insofar as the former complex is stabilized by a chlorine-shared halogen bond and the latter by a chlorine-transferred bond. Figure 6 once again illustrates that intermolecular distances can be extracted from values of two-bond coupling constants across the intermolecular interaction.

The data of Table S5 (Supporting Information) show that the FC term dominates $^{2X}J(\text{F-P})$ and is an excellent approximation to the total coupling constant for complexes with traditional halogen bonds. For FCl:PCLi with its chlorine-shared halogen bond, the FC term increases dramatically, and there is also an increase in the contribution of the SD term. When the bond becomes chlorine-transferred in FCl:PC^- , the FC term still dominates, but both the PSO and SD terms make non-negligible contributions.

$^{1X}J(\text{Cl-P})$. Values of the third coupling constant $^{1X}J(\text{Cl-P})$ are also reported in Table 5. This coupling constant tends to increase as the Cl-P distance decreases in complexes with traditional halogen bonds, exhibits a large increase in FCl:PCLi , but then decreases dramatically in the chlorine-transferred FCl:PC^- complex. Some insight into this behavior can be gained by considering the values of $^1J(\text{Cl-P})$ in the cation ClPCLi^+ and the molecule ClPC . Figure 7 illustrates the change in the Cl-P coupling constant in these systems as a function of the Cl-P distance. The gradual increase in $^{1X}J(\text{Cl-P})$ is evident for complexes with traditional halogen bonds, followed by a marked increase for the complex FCl:PCLi and then

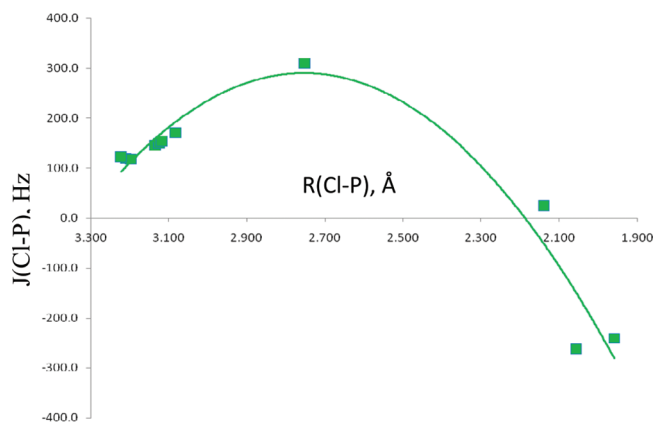


Figure 7. $^{1X}J(\text{Cl-P})$ for complexes FCl:PCX and $^1J(\text{Cl-P})$ for monomers ClPCLi^+ and ClPC versus the Cl-P distance. The correlation coefficient is 0.92.

decrease for FCl:PC^- . The values at the two shortest distances in Figure 7 are for the covalent bond in the reference cation and neutral molecule. From Figure 7 it is easy to see the dependence of the Cl-P coupling constant on the nature of the Cl-P bond, and how the small value of this coupling constant for the FCl:PC^- complex relates to the degree of transfer of the Cl atom to P, and to the covalent bond in the reference monomers. It should not be surprising that it is the FC term that reflects the degree of Cl transfer, as it changes from a positive value in the complexes to a large negative value in the cation and the neutral molecule. A negative value of a one-bond coupling constant in a molecule is often seen in the presence of lone pairs of electrons.

Spin-Spin Coupling Constants for Complexes with Configuration II. Coupling constants for four configuration II complexes, FCl:PCF , FCl:PCH , FCl:PCCH_3 , and FCl:PCLi , have also been computed, and are reported in Table 6. The components of these coupling constants are given in Table S6 of the Supporting Information.

$^1J(\text{F-Cl})$. As expected, $^1J(\text{F-Cl})$ decreases upon complexation as the F-Cl distance increases. $^1J(\text{F-Cl})$ values for configuration II complexes are less than those for configuration I complexes, a reflection of the longer F-Cl distances in configuration II. Moreover, when points for $^1J(\text{F-Cl})$ and the F-Cl distance for these four complexes are added to the corresponding data for the neutral configuration I complexes, $^1J(\text{F-Cl})$ varies quadratically with $R(\text{F-Cl})$ with a much improved correlation coefficient of 0.956, as illustrated in Figure 8. The improved correlation reflects in part the expanded scales for both variables. Patterns among the components of $^1J(\text{F-Cl})$ are similar to those observed for configuration I.

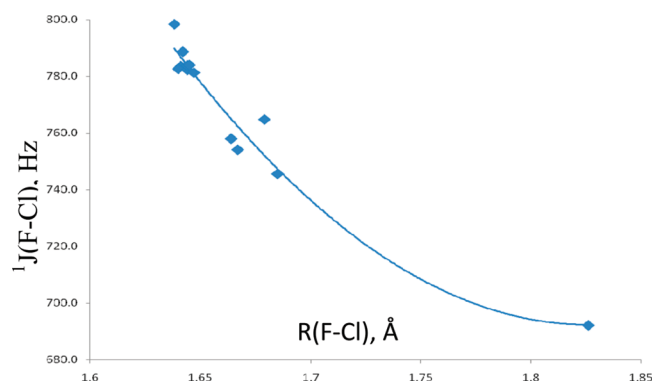
$^{2X}J(\text{F-P})$ and $^{2X}J(\text{F-C})$. Values of $^{2X}J(\text{F-P})$ and $^{2X}J(\text{F-C})$ across the $\text{F-Cl}\cdots\text{P}$ and $\text{F-Cl}\cdots\text{C}$ interactions for complexes with configuration II are also given in Table 6. The F-P distances in complexes with configuration II are significantly shorter than the F-P distances for the corresponding configuration I complexes, but $^{2X}J(\text{F-P})$ values across the $\text{F-Cl}\cdots\text{P}$ π interactions are dramatically reduced relative to those for $\text{F-Cl}\cdots\text{P}$ halogen bonds at the P lone pair. $^{2X}J(\text{F-P})$ for configuration II complexes correlates with the F-P distance, with a correlation coefficient of 0.999. However, this correlation is based on only four points, with three clustered together and the fourth corresponding to a complex in which the PCLi molecule is significantly distorted. Absolute values of $^{2X}J(\text{F-C})$ are less than 2 Hz.

The nature of F-P coupling in complexes with configuration II is essentially different from F-P coupling for configuration I. For configuration II complexes, the FC term is never the dominant term. Rather, for complexes FCl:PCF , FCl:PCH , and FCl:PCCH_3 , the negative PSO term has the largest absolute value followed by positive FC and SD terms that are similar. For the complex FCH:PCLi in which chlorine transfer occurs, the SD term is positive and makes the largest contribution, followed by a negative PSO term and a positive FC term that have comparable absolute values. It is the FC and SD terms together that make $^{2X}J(\text{F-P})$ large and positive.

Values of $^{1X}J(\text{Cl-P})$ for coupling across the $\text{F-Cl}\cdots\text{P}$ halogen bonds for configuration II complexes are significantly reduced relative to those for corresponding configuration I complexes, despite the shorter Cl-P distances in the former. Once again, this suggests that coupling through the perturbed π system is less efficient than coupling through the σ lone pair.

Table 6. Distances (*R*, Å) and One- and Two-Bond Coupling Constants (Hz) Across Halogen Bonds for Selected FCl:PCX Configuration II Complexes

| complex | <i>R</i> (F–Cl) | ¹ <i>J</i> (F–Cl) | <i>R</i> (Cl–P) | ¹ <i>XJ</i> (Cl–P) | <i>R</i> (F–P) | ² <i>XJ</i> (F–P) | <i>R</i> (Cl–C) | ¹ <i>XJ</i> (Cl–C) | <i>R</i> (F–C) | ² <i>XJ</i> (F–C) |
|-----------------------|-----------------|------------------------------|-----------------|-------------------------------|----------------|------------------------------|-----------------|-------------------------------|----------------|------------------------------|
| FCl:PCF | 1.664 | 757.9 | 3.005 | 52.6 | 4.656 | −7.1 | 2.803 | 7.1 | 4.389 | −0.4 |
| FCl:PCH | 1.667 | 754.1 | 3.032 | 45.2 | 4.664 | −4.3 | 2.724 | −1.5 | 4.350 | −1.5 |
| FCl:PCCH ₃ | 1.685 | 745.5 | 2.889 | 64.8 | 4.549 | 2.4 | 2.650 | 13.9 | 4.269 | −0.4 |
| FCl:PCLi | 1.826 | 692.1 | 2.626 | 89.4 | 4.425 | 81.7 | 2.374 | 33.1 | 4.107 | 0.0 |

**Figure 8.** ¹*J*(F–Cl) versus the F–Cl distance for complexes with configuration I and II. The correlation coefficient is 0.956.

Both ¹*XJ*(Cl–P) and ¹*XJ*(Cl–C) increase as the corresponding distances decrease. However, Cl–C coupling in configuration II complexes should not be compared with Cl–C coupling in configuration I complexes, because Cl and C are not bonded in configuration I. The FC term is the dominant term for both ¹*XJ*(Cl–P) and ¹*XJ*(Cl–C).

CONCLUSIONS

Ab initio MP2/aug'-cc-pVTZ calculations have been performed to investigate the halogen-bonded complexes FCl:PCX, for X = NC, CN, F, H, CCH, CCF, CH₃, Li, and Na. The results of these calculations support the following statements.

1. Some stable complexes exist which have F–Cl...P halogen bonds formed through the lone pair at P (configuration I). However, with one exception, the more stable FCl:PCX complexes involve interaction of FCl with the C≡P triple bond through the perturbed π system (configuration II).
2. Neutral configuration I complexes with traditional halogen bonds have binding energies between 5 and 10 kJ/mol. FCl:PCLi and FCl:PCNa are stabilized by chlorine-shared halogen bonds, with binding energies of 23 and 28 kJ/mol, respectively. FCl:PC[−] undergoes chlorine transfer to form a chlorine-transferred halogen bond with a binding energy of 128 kJ/mol relative to FCl and PC[−]. Thus, the type of halogen bond changes from traditional, to chlorine-shared, to chlorine-transferred as the electron-donating ability of the substituent increases.
3. All complexes FCl:PCX except FCl:PCCN have the π complex (II) as the more stable minimum on the potential surface. Complexes X = NC, F, H, CCH, CCF, and CH₃ have binding energies that range from 16 to 29 kJ/mol. The binding energies of FCl:PCLi and FCl:PCNa are significantly higher at 79 and 158 kJ/mol, respectively. These high binding energies arise from the chlorine-transferred nature of the halogen bonds,

which results in significant distortion of the PCLi and PCNa molecules.

4. The SAPT analysis indicates that the most stabilizing term for configuration I complexes with traditional halogen bonds is the dispersion interaction. The electrostatic interaction is the most important SAPT term for configuration I complexes with chlorine-shared halogen bonds. The most important term for configuration II complexes is the electrostatic interaction, except for FCl:PCNa for which the induction term is the most important.
5. The F–Cl stretching frequency is red-shifted in all complexes relative to the FCl monomer. This shift is greater for complexes with configuration II, and correlates linearly with the increase in the F–Cl distance upon complexation.
6. EOM-CCSD/(qzp,qz2p) spin–spin coupling constants ¹*J*(F–Cl), ¹*XJ*(Cl–P), and ²*XJ*(F–P) have been computed for configuration I complexes. ¹*J*(F–Cl) decreases upon complexation. Values of ²*XJ*(F–P) exhibit a quadratic dependence on the F–P distance and are very sensitive to halogen bond type. ¹*XJ*(Cl–P) tends to increase as the Cl–P distance decreases, exhibits a large increase for FCl:PCLi, but then decreases in the chlorine-transferred FCl:PC[−] complex. The decrease in ¹*XJ*(Cl–P) in this complex is consistent with values of ¹*J*(Cl–P) for the covalent Cl–P bond in ClPCLi⁺ and ClPC.
7. ¹*J*(F–Cl) coupling constants decrease to a greater extent for configuration II complexes compared to configuration I, a reflection of the longer F–Cl distances in II. Despite shorter F–P and Cl–P distances in configuration II, ²*XJ*(F–P) and ¹*XJ*(Cl–P) values are significantly reduced relative to those for configuration I. The nature of the F–P coupling is dramatically different in configurations I and II, as evidenced by the relative importance of PSO, FC, and SD components.

ASSOCIATED CONTENT

Supporting Information

Total energies and geometries of complexes, SAPT energies, electron densities and Laplacians at bond critical points, and PSO, DSO, FC, and SD components of coupling constants. This material is available free of charge via the Internet at <http://pubs.acs.org>.

AUTHOR INFORMATION

Corresponding Author

*E-mails: I.A., ibon@iqm.csic.es; J.E.D.B., jedelbene@ysu.edu.

Notes

The authors declare no competing financial interest.

ACKNOWLEDGMENTS

Thanks are due to the Ohio Supercomputer Center for continuing support of this research. We also thank the Ministerio de Ciencia e Innovación (Project No. CTQ2009-13129-C02-02), and the Comunidad Autónoma de Madrid (Project MADRISOLAR2, ref S2009/PPQ-1533) for continuing support. Thanks are also given to the CTI (CSIC) for an allocation of computer time.

REFERENCES

- (1) Gier, T. E. *J. Am. Chem. Soc.* **1961**, *83*, 1769.
- (2) (a) Kaye, J. A.; Strobel, D. F. *Icarus* **1984**, *59*, 314. (b) Turner, B. E.; Tsuji, T.; Bally, J.; Guelin, M.; Cernicharo, J. *Astrophys. J.* **1990**, *365*, 569. (c) MacKay, D. D. S.; Charnley, S. B. *Mon. Not. R. Astron. Soc.* **2001**, *325*, 545. (d) Agúndez, M.; Cernicharo, J.; Guélin, M. *Astrophys. J.* **2007**, *662*, L91.
- (3) Ishikawa, H.; Toyosaki, H.; Mikami, N.; Pérez-Bernal, F.; Vaccaro, P. H.; Iachello, F. *Chem. Phys. Lett.* **2002**, *365*, 57.
- (4) Regitz, M. *Chem. Rev.* **1990**, *90*, 191.
- (5) (a) Nguyen, M. T. *J. Chem. Soc., Chem. Commun.* **1990**, 989. (b) Nguyen, M. T.; Landuyt, L.; Vanquickenborne, L. G. *J. Org. Chem.* **1993**, *58*, 2817. (c) Creve, S.; Nguyen, M. T.; Vanquickenborne, L. G. *Eur. J. Inorg. Chem.* **1999**, 1281.
- (6) (a) Geissler, B.; Barth, S.; Bergsträsser, U.; Slany, M.; Durkin, J.; Hitchcock, P. B.; Hofmann, M.; Binger, P.; Nixon, J. F.; Schleyer, P. v. R.; Regitz, M. *Angew. Chem., Int. Ed.* **1995**, *34*, 484. (b) Hofmann, M.; Schleyer, P. v. R.; Regitz, M. *Eur. J. Org. Chem.* **1999**, 3291.
- (7) Johns, J. W. C.; Shurvell, H. F.; Tyler, J. K. *Can. J. Phys.* **1969**, *47*, 893.
- (8) (a) Strey, G.; Mills, I. M. *Mol. Phys.* **1973**, *26*, 129. (b) Garneau, J. M.; Cabana, A. J. *Mol. Spectrosc.* **1978**, *69*, 319. (c) Garneau, J. M.; Cabana, A. J. *Mol. Spectrosc.* **1981**, *87*, 490. (d) Murrell, J. N.; Carter, S.; Halonen, L. O. *J. Mol. Spectrosc.* **1982**, *93*, 307. (e) Ohno, K.; Matsuura, H.; Murata, H. *J. Mol. Spectrosc.* **1983**, *100*, 403. (f) Jung, M.; Winnewiesser, B. P.; Winnewiesser, M. *J. Mol. Struct.* **1997**, *413–414*, 31. (g) Beck, C.; Schinke, R.; Koput, J. *J. Chem. Phys.* **2000**, *112*, 8446.
- (9) Kalasinsky, V. F.; Pechsin, S. J. *Raman Spectrosc.* **1985**, *16*, 190.
- (10) Tyler, J. K. *J. Chem. Phys.* **1964**, *40*, 1170.
- (11) Johns, J. W.; Stone, J. M. R.; Winnewiesser, G. *J. Mol. Spectrosc.* **1971**, *38*, 437.
- (12) (a) Chen, Y. T.; Watt, D. M.; Field, R. W.; Lehmann, K. K. *J. Chem. Phys.* **1990**, *93*, 2149. (b) Ishikawa, H.; Nagao, C.; Mikami, N.; Field, R. W. *J. Chem. Phys.* **1997**, *106*, 2980.
- (13) (a) Anderson, S. P.; Goldwhite, H.; Ko, D.; Letsou, A.; Esparza, F. *J. Chem. Soc., Chem. Commun.* **1975**, 744. (b) Pellerin, B.; Denis, J. M.; Perrocheau, J.; Carrié, R. *Tetrahedron Lett.* **1986**, *27*, 5723. (c) Guillemin, J. C.; Janati, T.; Guenot, P.; Savignac, P.; Denis, J. M. *Angew. Chem., Int. Ed.* **1991**, *30*, 196. (d) Hübler, K.; Schwerdtfeger, P. *Inorg. Chem.* **1999**, *38*, 157.
- (14) Thomson, C. *Theor. Chim. Acta* **1974**, *35*, 237.
- (15) Karna, S. P.; Bruna, P. J.; Grein, F. *Can. J. Phys.* **1990**, *68*, 499.
- (16) Nguyen, M. T.; Ka, T. K. *J. Mol. Struct. (THEOCHEM)* **1986**, *139*, 145.
- (17) Ma, N. L.; Wong, S. S.; Paddon-Row, M. N.; Li, W. K. *Chem. Phys. Lett.* **1993**, *213*, 189.
- (18) Goldstein, E.; Jin, S.; Carrillo, M. R.; Cave, R. J. *J. Comput. Chem.* **1993**, *14*, 186.
- (19) Lohr, L. L. *J. Mol. Spectrosc.* **1993**, *162*, 300.
- (20) Ingels, J. B.; Turney, J. M.; Richardson, N. A.; Yamaguchi, Y.; Schaefer, H. F., III. *J. Chem. Phys.* **2006**, *125*, 104306.
- (21) Del Bene, J. E.; Alkorta, I.; Elguero, J. *Chem. Phys. Lett.* **2006**, *429*, 23.
- (22) Alkorta, I.; Elguero, J.; Del Bene, J. E. *J. Phys. Chem. A* **2007**, *111*, 9924.
- (23) Del Bene, J. E.; Alkorta, I.; Elguero, J. *J. Phys. Chem. A* **2010**, *114*, 8463.
- (24) Del Bene, J. E.; Alkorta, I.; Elguero, J. *Chem. Phys. Lett.* **2011**, *508*, 6.
- (25) Del Bene, J. E.; Alkorta, I.; Elguero, J. *J. Phys. Chem. A* **2010**, *114*, 12958.
- (26) Del Bene, J. E.; Alkorta, I.; Elguero, J. *Phys. Chem. Chem. Phys.* **2011**, *13*, 13951.
- (27) Del Bene, J. E. *J. Phys. Chem.* **1993**, *97*, 107.
- (28) Dunning, T. H., Jr. *J. Chem. Phys.* **1989**, *90*, 1007.
- (29) Woon, D. E.; Dunning, T. H., Jr. *J. Chem. Phys.* **1995**, *103*, 4572.
- (30) Frisch, M. J.; Trucks, G. W.; Schlegel, H. B.; Scuseria, G. E.; Robb, M. A.; Cheeseman, J. R.; Scalmani, G.; Barone, V.; Mennucci, B.; Petersson, G. A.; Nakatsuji, H.; Caricato, M.; Li, X.; Hratchian, H. P.; Izmaylov, A. F.; Bloino, J.; Zheng, G.; Sonnenberg, J. L.; Hada, M.; Ehara, M.; Toyota, K.; Fukuda, R.; Hasegawa, J.; Ishida, M.; Nakajima, T.; Honda, Y.; Kitao, O.; Nakai, H.; Vreven, T.; Montgomery, J. A., Jr.; Peralta, J. E.; Ogliaro, F.; Bearpark, M.; Heyd, J. J.; Brothers, E.; Kudin, K. N.; Staroverov, V. N.; Kobayashi, R.; Normand, J.; Raghavachari, K.; Rendell, A.; Burant, J. C.; Iyengar, S. S.; Tomasi, J.; Cossi, M.; Rega, N.; Millam, N. J.; Klene, M.; Knox, J. E.; Cross, J. B.; Bakken, V.; Adamo, C.; Jaramillo, J.; Gomperts, R.; Stratmann, R. E.; Yazyev, O.; Austin, A. J.; Cammi, R.; Pomelli, C.; Ochterski, J. W.; Martin, R. L.; Morokuma, K.; Zakrzewski, V. G.; Voth, G. A.; Salvador, P.; Dannenberg, J. J.; Dapprich, S.; Daniels, A. D.; Farkas, Ö.; Foresman, J. B.; Ortiz, J. V.; Cioslowski, J.; Fox, D. J. *Gaussian 09, Revision A.1*; Gaussian, Inc.: Wallingford, CT, 2009.
- (31) Jeziorski, B.; Moszynski, R.; Szalewicz, K. *Chem. Rev.* **1994**, *94*, 1887.
- (32) Misquitta, A. J.; Podeszwa, R.; Jeziorski, B.; Szalewicz, K. *J. Chem. Phys.* **2005**, *123*, 214103.
- (33) Heßelmann, A.; Jansen, G. *Phys. Chem. Chem. Phys.* **2003**, *5*, 5010.
- (34) Moszynski, R.; Heijmen, T. G. A.; Jeziorski, B. *Mol. Phys.* **1996**, *88*, 741.
- (35) Werner, H.-J.; Knoles, P. J.; Manby, F. R.; Schutz, M.; et al. *MOLPRO, a package of ab initio programs*, version 2010.1; see <http://www.molpro.net>.
- (36) Perdew, J. P.; Burke, K.; Ernzerhof, M. *Phys. Rev. Lett.* **1996**, *77*, 3865.
- (37) Bader, R. F. W. *Atoms in Molecules: A Quantum Theory*; The International Series of Monographs of Chemistry; Halpen, J., Green, M. L. H., Eds.; Clarendon Press: Oxford, U.K., 1990.
- (38) Popelier, P. L. A. *Atoms in Molecules: An Introduction*; Prentice Hall: Englewood Cliffs, NJ, 2000.
- (39) Keith, T. A. *AIMAll*, Version 08.11.29; 2008; aim.tkgristmill.com.
- (40) Noury, S.; Krokidis, X.; Fuster, F.; Silvi, B. *ToPMoD*; Université Pierre et Marie Curie: Paris, 1999.
- (41) Silvi, B.; Savin, A. *Nature* **1994**, *371*, 683.
- (42) Perera, S. A.; Sekino, H.; Bartlett, R. J. *J. Chem. Phys.* **1994**, *101*, 2186.
- (43) Perera, S. A.; Nooijen, M.; Bartlett, R. J. *J. Chem. Phys.* **1996**, *104*, 3290.
- (44) Schäfer, A.; Horn, H.; Ahlrichs, R. *J. Chem. Phys.* **1992**, *97*, 2571.
- (45) Del Bene, J. E.; Elguero, J.; Alkorta, I.; Yañez, M.; Mó, O. *J. Phys. Chem. A* **2006**, *110*, 9959.
- (46) Kirpekar, S.; Jensen, H. J. A.; Oddershede, J. *Chem. Phys.* **1994**, *188*, 171.
- (47) ACES II is a program product of the Quantum Theory Project, University of Florida. Authors: Stanton, J. F.; Gauss, J.; Watts, J. D.; Nooijen, M.; Oliphant, N.; Perera, S. A.; Szalay, P. G.; Lauderdale, W. J.; Gwaltney, S. R.; Beck, S.; Balkova, A.; Bernholdt, D. E.; Baeck, K.-K.; Tozyczko, P.; Sekino, H.; Huber, C.; Bartlett, R. J. Integral packages included are VMOL (Almlöf, J.; Taylor, P. R.), VPROPS (Taylor, P. R.), ABACUS (Helgaker, T.; Jensen, H. J. A.; Jorgensen, P.; Olsen, J.; Taylor, P. R.). Brillouin–Wigner perturbation theory was implemented by Pittner, J.
- (48) Alkorta, I.; Rozas, I.; Elguero, J. *Theor. Chem. Acc.* **2007**, *118*, 533.

- (49) Linstrom, P. J.; Mallard, W. G., Eds. In *NIST Chemistry Webbook*; NIST Standard Reference Database No. 69; National Institute of Standards and Technology: Gaithersburg, MD, 2003; <http://webbook.nist.gov>.
- (50) Mata, I.; Alkorta, I.; Molins, E.; Espinosa, E. *Chem.—Eur. J.* **2010**, *16*, 2442.
- (51) Alkorta, I.; Zborowski, K.; Elguero, J.; Solimannejad, M. J. *Phys. Chem. A* **2006**, *110*, 10279.
- (52) Alkorta, I.; Elguero, J. *Struct. Chem.* **2004**, *15*, 117.
- (53) Irikura, K. K. *J. Phys. Chem. Ref. Data, Suppl. 1* **1985**, *14*, 1.
- (54) Del Bene, J. E.; Jordan, M. J. T. Vibrational Spectroscopy of the Hydrogen Bond: An Ab Initio Quantum Chemical Perspective. *Int. Rev. Phys. Chem.* **1999**, *18*, 119.
- (55) Del Bene, J. E.; Elguero, J. In *Computational Chemistry: Reviews of Current Trends*; Leszczynski, J., Ed.; World Scientific Publishing Co. Pte, Ltd.: Singapore, 2006; Vol. 10, pp 229–264.